Available online at www.sciencedirect.com
ScienceDirect
Journal of Photochemistry and Photobiology B: Biology xxx (2006) xxx–xxx
Journal of Photochemistry and Photobiology B:Biology
www.elsevier.com/locate/jphotobiol

Short communication

Ultrastructural and autoradiographical analysis show a faster skin repair in He–Ne laser-treated wounds

Carlos E.N. de Araújo [a], Martha S. Ribeiro [b], Rodolfo Favaro [a], Denise M. Zezell [b], Telma M.T. Zorn [a,*]

[a] *Department of Cell and Development Biology, Institute of Biomedical Sciences, University of São Paulo, Av. Lineu Prestes, 1524, 05508-000 São Paulo, São Paulo, Brazil*
[b] *Center for Lasers and Applications, Institute of Nuclear and Energetic Researches, IPEN-CNEN/SP, São Paulo, Brazil*

Received 31 March 2006; received in revised form 31 July 2006; accepted 7 August 2006

Abstract

There are evidences that low-intensity red laser radiation is capable to accelerate wound healing. Nowadays, this therapy has been gradually introduced in clinical practice although mechanisms underlying laser effects are poorly understood. To better understand the photobiological effects of laser radiation, this study investigated by electron microscopy, immunohistochemistry and autoradiography the morphological and functional features of irradiated and none irradiated injured mice skin. Full-thickness skin lesions were created on the back of mice and irradiated on days 1, 5, 8, 12, and 15 post-wounding with a He–Ne laser ($\lambda = 632.8$ nm), dose 1 J/cm^2, exposure time 3 min. Non-irradiated lesions were used as a control. The mice were inoculated with ^{3}H-proline and sacrificed one hour after on the 8th, 15th and 22nd days to histological and radioautographical analysis. The irradiated-lesions showed a faster reepithelization compared with control lesions. The irradiated dermis contained a higher number of activated fibroblasts compared to control group and, most of them showed several cytoplasmic collagen-containing phagosomes. In irradiated-lesions, smooth muscle α-actin positive cells predominated, which correspond to a higher number of myofibroblasts observed in the electron microscope. Moreover, laser radiation reduced the local inflammation and appears to influence the organization of collagen fibrils in the repairing areas. Quantitative autoradiography showed that the incorporation of ^{3}H-proline was significantly higher in irradiated-dermis on the 15th day post-wounding ($p < 0.05$). These results suggest that laser radiation may accelerate cutaneous wound healing in a murine model.

Keywords: 633 nm wavelength; Low-intensity laser therapy; Mice; Wound healing

1. Introduction

There has been recently an increased interest in the use of low-intensity red and near infrared laser radiation to accelerate wound healing and tissue regeneration. Photobiological responses are the result of photochemical and/or photophysical changes produced by absorption of non-ionizing electromagnetic radiation [1]. Some studies have reported beneficial effects of laser biostimulation on wound healing in cell cultures as well as in animal models [2–6]. Nowadays, this therapy is successfully applied in clinical practice although the mechanisms underlying laser effects are still poorly understood.

Indications exist that low-intensity laser therapy (LILT) stimulates collagen production by cultured skin fibroblasts [7,8] and increases procollagen type I and type III mRNA in skin wounds [9]. Macrophage stimulation has also been observed both *in vitro* and *in vivo* studies [10,11], however, *in vivo* quantitative morphological studies have rarely been performed.

It is established that wound healing is a controlled biological process that comprises complexes cell–cell and cell–extracellular matrix interactions [12]. Therefore, the study

* Corresponding author. Tel./fax: +55 11 3091 7309.
E-mail address: temtzorn@usp.br (T.M.T. Zorn).

1011-1344/$ - see front matter © 2006 Published by Elsevier B.V.
doi:10.1016/j.jphotobiol.2006.08.006

of healing process requires the understanding of cellular behavior and its interactions with the surrounding extracellular matrix (ECM). The sequence of events that culminate in a complete wound closure and repair can be divided into three overlapping phases: inflammation, reepithelization and ECM remodeling, which begin almost simultaneously with reepithelization. The quality of wound healing, however, depends on a fine equilibrium between collagen formation and degradation.

Electron microscopy and autoradiography constitute powerful instruments to perform high-resolution morphological and physiological quantitative studies. Further, the immunohistochemistry helps the identification of gene products, and allows a better characterization of the cell types. Nevertheless, these tools have been rarely employed to investigate the effect of LILT on cutaneous wound healing. The present study is an ultrastructural, immunohistochemical and autoradiographic evaluation of mouse skin during the healing process stimulated by low-intensity He–Ne laser radiation.

2. Materials and methods

Thirty Swiss male adult mice with body mass of about 30 g were used. During the experimental period, all animals were kept in individual cages in a 12 h light/ 12 h-darkness schedule at 22 °C with granulated ration and water *ad libitum*. The animals were anesthetized by intraperitoneal injection of Avertin® (0.025 mL/g). After anesthesia, the surgical site was shaved and two standardized 6-mm-diameter round full-thickness wounds were made on the median region of the back by means of a punch-skin biopsy device. Institute of Biomedical Science Animal Ethics Committee approved the experiments (authorization number 144/2002).

Considering the individual variability of skin repair, irradiated and non-irradiated lesions were created in the same animal separated by 1 cm from each other. Therefore, each experimental animal acted as its own control. The experimental lesion was irradiated with a He–Ne laser (UNIPHASE, USA) with a wavelength of $\lambda = 632.8$ nm, 10 mW of output power and a beam diameter about 2 mm. The beam was expanded to 6 mm by an objective ($f = 7$ cm) and a neutral density filter 0.04 for $\lambda = 632.8$ nm was used to ensure a uniform exposition of the entire lesion. The dose used was 1 J/cm^2 per irradiation corresponding to an exposure time of 3 min, which was calculated by the lesion area [3,13,14]. The lesions that were not irradiated were considered the control group. Lesions were randomly divided into laser or control group.

The laser group lesions were irradiated on the 1st, 5th, 8th, 12th, and 15th day post-wounding (p.w.). Animals were sacrificed by cervical dislocation on the 8th, 15th and 22nd days p.w. To allow a rational use of the animals and also to get results from the same experimental animal, before the sacrifice, the animals were injected intraperitoneally (i.p.) with tritiated proline according to the protocol described below in this chapter. Two circular skin biopsies with 8-mm-diameter containing the total dermis were carefully collected. Each sample was divided into two parts. One section was used for electron-microscopy studies, and the other destined to light microscope studies including autoradiography and immunohistochemistry.

2.1. Electron microscopy

Skin fragments were fixed by immersion in a solution of 2% glutaraldehyde and 2% paraformaldehyde in 0.125 M sodium cacodylate buffer at pH 7.4 [15]. After washing, the tissues were post-fixed with 1% osmium tetroxide in 0.1 M sodium phosphate, pH 7.4 for 1 h, dehydrated in graded ethanol, and thereafter embedded in Spurr resin. One-micrometer sections were stained with 0.25% toluidine blue for 30 s, and observed with a Nikon Labophot AFX-II light microscope. Representative areas were selected, and cut at 50-nm-thickness, stained with uranyl acetate and lead citrate. After the staining process, the samples were observed with a JEOL 100CX II electron microscope15.

2.2. Immunohistochemistry

Skin samples were fixed in Bouin's fixative for 24 h at room temperature, dehydrated and embedded in paraffin. Five-micrometer sections were cut in a microtome (Microm HM-200), adhered to glass slides using 0.1% poly-L-lysine (Sigma, USA) and then air-dried at room temperature. Each of the succeeding steps was followed by a thorough rinse with PBS.

All steps were performed in a humid chamber at room temperature and care was taken to avoid drying of the sections. To block endogenous peroxidase activity, sections were treated with 3% H_2O_2 (Merck) in phosphate-buffered saline (PBS) for 30 min. Non-specific reaction was blocked by incubating the section for 30 min with normal goat serum diluted 1:1 in PBS-10% bovine serum albumin. Sections were incubated overnight at 4 °C in rabbit anti-smooth muscle α-actin IgG (alpha-SMA) (Sigma, USA) diluted in PBS-0.3% Tween 20, and washed thoroughly with PBS, then incubated with biotinylated goat anti-rabbit IgG (Vector Labs, Burlingame, CA, USA) diluted 1:1000 in PBS for 1 h at room. After extensive rinsing in PBS, all sections were treated with streptavidin/peroxidase (Vectastain ABC kit, Vector Labs) for 1 h at room temperature. The reaction was visualized using 0.03% 3,3′-diaminobenzidine (Sigma, USA) plus 0.03% H_2O_2 in PBS. After immunostaining, sections were lightly stained with Meyer's hematoxylin. For each immunohistochemical reaction, controls were performed by omitting the primary antibody. The samples were examined with a Nikon Eclipse E600 microscope. Images were captured using the Image Pro Plus software computer program (Media Cybernetics, Silver Spring, MD, USA). Alpha-SMA- positive cells were evaluated by counting immunoreactive cells present in a total of 10 squares each one measuring 10,000 μm^2.

Please cite this article as: Carlos E.N. de Araújo et al., Ultrastructural and autoradiographical analysis show a faster ..., Journal of Photochemistry and Photobiology B: Biology (2006), doi:10.1016/j.jphotobiol.2006.08.006

2.3. Autoradiography

On days 8, 15, and 22 p.w., the animals were injected i.p. with 5 μCi/g of body mass of ^{3}H-proline and killed 1 h later by cervical dislocation.

After sacrifice, the wounds were removed and fixed in Bouin's fixative for 24 h as described for immunohistochemistry procedure. Five-micrometer sections were mounted on glass slides, dehydrated and coated in dark chamber, with K2 nuclear emulsion (Ilford, England) by dipping method [16]. After exposure at 4 °C for 30 days, the autoradiograms were photographically developed in D19b developer (Kodak, USA), fixed and stained with hematoxylin and eosin. The incorporation of ^{3}H-proline was evaluated by counting silver granules in 20 selected areas of the central repairing region of the dermis.

Silver grains in autoradiograms as well as alpha-SMA-positive cells were semi-automatically counted using the Image ProPlus software (Medio Cybernetics, Maryland, USA). The average and standard errors (SE) were computed. The differences between control and treated groups were analyzed by using Student *t*-test. Significance was accepted at $p < 0.05$.

3. Results

3.1. Light microscopy

On day 8 p.w., control group presented wound edges still open while the irradiated-lesions were reepithelized. Particularly in control group, the injured dermis showed signals of inflammatory activity evidenced by the presence of a great number of leukocytes, mainly neutrophils (Fig. 1A and B). In irradiated samples some fibroblast were seen in mitosis.

After 15 days p.w., both irradiated and control lesions were completely recovered by a new epidermis. The inflammatory response was diminished in the irradiated-lesions, but it remained in a certain degree in control lesions. In both irradiated and control lesions the fibroblasts were larger than that ones existent in the peripheral of the non-injured dermis (Fig. 1C and D).

After 22 days p.w., irradiated and control lesions were completely recovered by a thick epithelial layer. The repaired dermis was easily distinguished from the original ones by the absence of glands and hair follicles, by the great number of large fibroblasts and by the organization of extracellular matrix. In both lesions, the inflammatory cells were rare (Fig. 1E and F).

3.2. Ultrastructure

On day 8 p.w., control group presented an intense inflammatory activity evidenced by the presence of a great number of leukocytes, mainly neutrophils. The ECM was mainly composed of short fragments of collagen fibrils scattered throughout the intercellular space (Fig. 2A). At the same period, the irradiated-lesions were completely reepithelized and showed less intense inflammatory activity than control samples. The predominant cell type was large

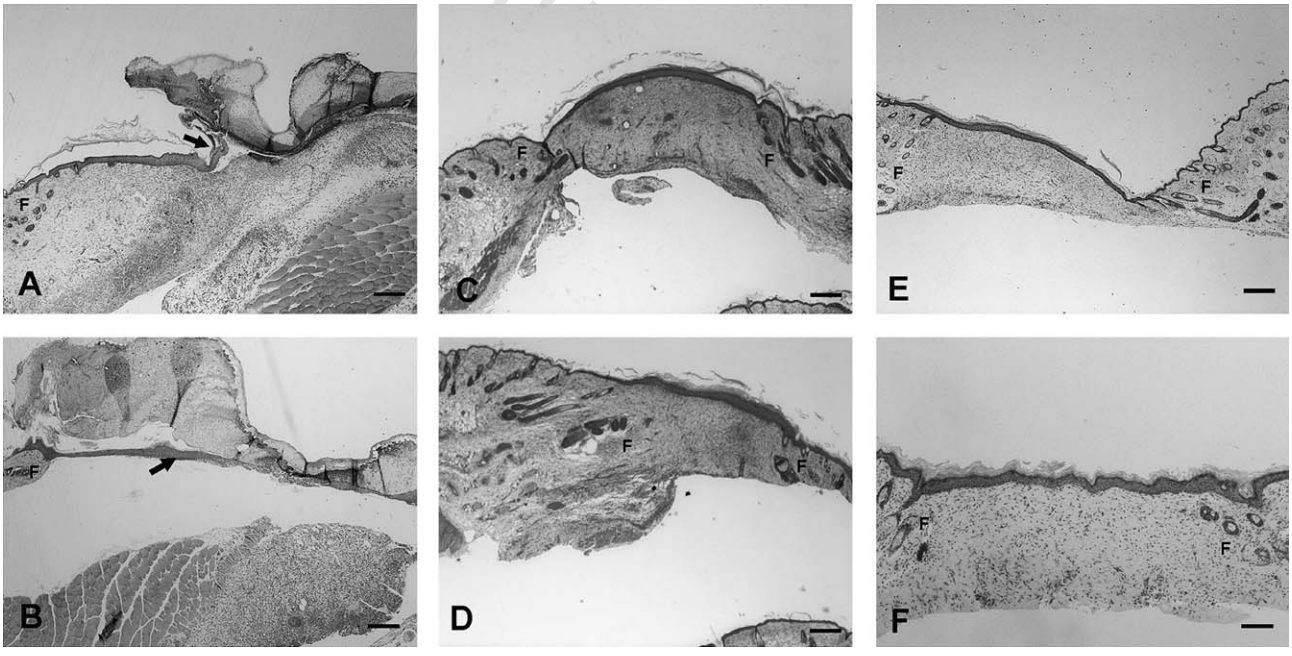

Fig. 1. (A–F) Photomicrograph of mouse skin. (A) Control dermis on day 8 p.w. Wound edge partially recovered by a thick epithelial layer (arrow) growing under the crust through the other side of the wound. Note hair follicles (F) present only in the normal skin. (B) Irradiated dermis on day 8 p.w. Observe the new epithelial layer recovering almost completely the injured dermis (arrow). (C) Control dermis on day 15 p.w. (D) Irradiated dermis on day 15 p.w. Both control and irradiated skin show a renewed dermis devoid of hair follicles. (E) Control dermis on day 22 p.w. (F) Irradiated dermis on day 22 p.w. The wound is completely reepithelized. Note that the epithelial layer of the irradiated skin is thicker than in the control skin. Bar scale: 250 μm.

Please cite this article as: Carlos E.N. de Araújo et al., Ultrastructural and autoradiographical analysis show a faster ..., Journal of Photochemistry and Photobiology B: Biology (2006), doi:10.1016/j.jphotobiol.2006.08.006

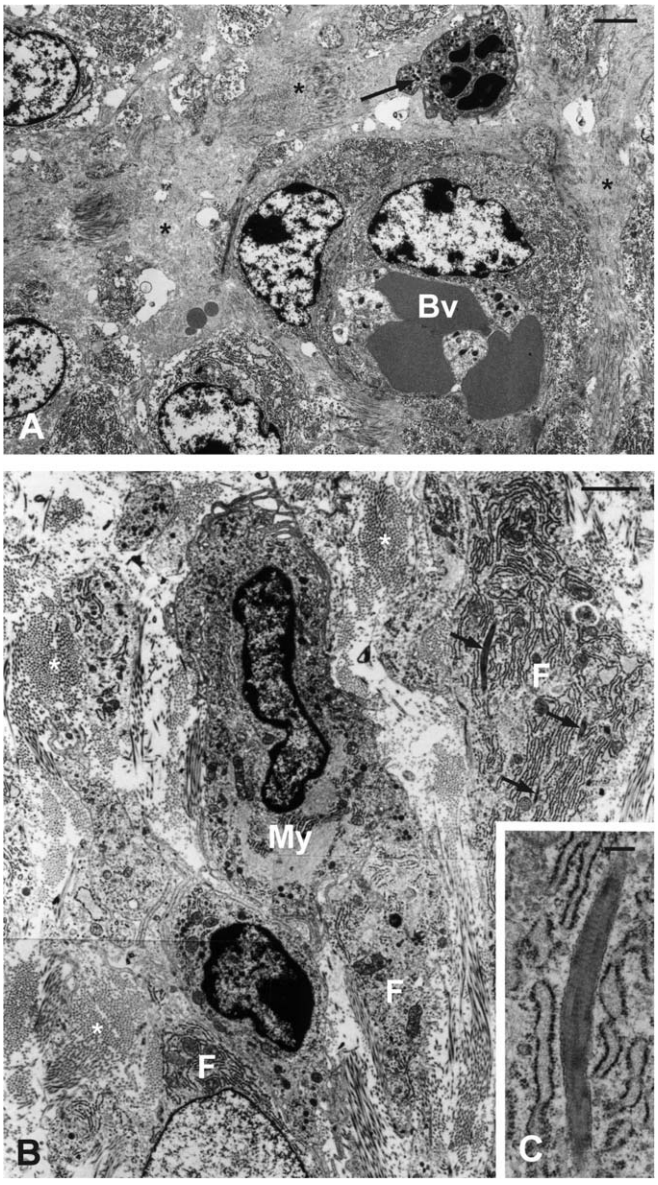

Fig. 2. (A) Control dermis on day 8 post-wounding (p.w). Note the intense inflammatory activity indicated by the polymorphonuclear infiltration (arrow). The extracellular matrix is composed by unorganized short collagen fibrils segments (*). Bv: blood vessel. Bar scale: 2 μm; (B and C) Irradiated dermis on day 8 p.w. (B) Photomontage of four electron micrographs showing fibroblasts with abundant and well-developed RER (F). These cells also contain phagocytosed collagen fibrils (arrow). Bundles of collagen fibrils fill the extracellular spaces (*). Observe a myofibroblast containing a rich network of microfilaments (My). Bar scale: 2 μm. (C) The insert shows a high magnification of a collagen-containing phagosome. Bar scale: 0.25 μm.

fibroblasts exhibiting an euchromatic nucleus and conspicuous nucleolus. The majority of fibroblasts were rich in rough endoplasmic reticulum (RER) with dilated lumen filled with electron-dense material, and exhibited large amounts of phagosome-containing collagen fibrils (Fig. 2B and C). These cells were usually surrounded by a loose ECM containing disperse thin collagen fibrils. Some myofibroblasts, identified by the high amount of cytoplasmic microfilaments and typical irregular nucleus, were present particularly in the deep dermis (Fig. 2B).

After 15 days p.w., the inflammatory response was decreased in the control lesions. In general, at this period, the extracellular matrix organization was similar to that of irradiated-lesions on day eight p.w. Fibroblasts were large and contained well-developed RER. Some of the fibroblasts showed cytoplasmic collagen-containing phagosomes. Phagocytosed collagen fibrils were clearly recognized by their typical transverse bands and they were frequently surrounded by an electron dense material similar to that observed in lysosomes. The ECM contained short segments of collagen fibrils, which in some places were arranged in small-unorganized bundles. In other areas, however, collagen fibrils were loose in packed (Fig. 3A). Some areas were devoid of collagen fibrils indicating the occurrence of edema (Fig. 3B).

Irradiated dermis contained many typical myofibroblasts characterized by the abundance of cytoplasmic microfilaments and indented nucleus (Fig. 3C). Besides myofibroblasts, typical fibroblasts with enlarged endoplasmic reticulum filled by electron-dense material were also present (Fig. 3D). Groups of thin and parallel collagen fibrils were involved by fibroblast cytoplasmic recesses (Fig. 3E). Remaining extracellular spaces were filled by bundles of well-organized collagen fibrils. The edema was reduced compared with the control lesions.

In the control lesions, most of the fibroblasts showed a well-developed RER with its cisterna fulfilled by electron-dense material (Fig. 4A). Many of the thin collagen fibrils were concentrated close to the fibroblasts surface. A diffuse edema continued to be observed indicating a persistent local inflammatory activity (Fig. 4B).

In the irradiated-lesions fibroblasts had abundant RER and were surrounded by an expressive amount of thin and well-organized collagen fibrils. Interestingly, on this day cytoplasmic recesses were no longer observed in fibroblasts (Fig. 4C). Numerous myofibroblasts continued to be observed. These cells showed many cytoplasmic projections and were orientated parallel to the surface of the skin. Edema was discrete and was restricted to superficial dermis (Fig. 4D).

3.3. Immunohistochemistry

Alpha-SMA-containing cells were detected in the dermis of both control and irradiated skin. However, the number of positive cells varied between the two groups and according to the period of skin repair.

Qualitative evaluation showed a higher number of alpha-SMA-positive cells in irradiated dermis than in the control dermis of the eighth day (Fig. 5A and B). In both days 15 and 22 p.w., alpha-SMA-positive cells predominate in the control dermis although irradiated samples still have some immunostained cells (Fig. 5C–F).

Fig. 6 displays the average of alpha-SMA-positive cells ± SE of both laser and control groups during experi-

Please cite this article as: Carlos E.N. de Araújo et al., Ultrastructural and autoradiographical analysis show a faster ..., Journal of Photochemistry and Photobiology B: Biology (2006), doi:10.1016/j.jphotobiol.2006.08.006

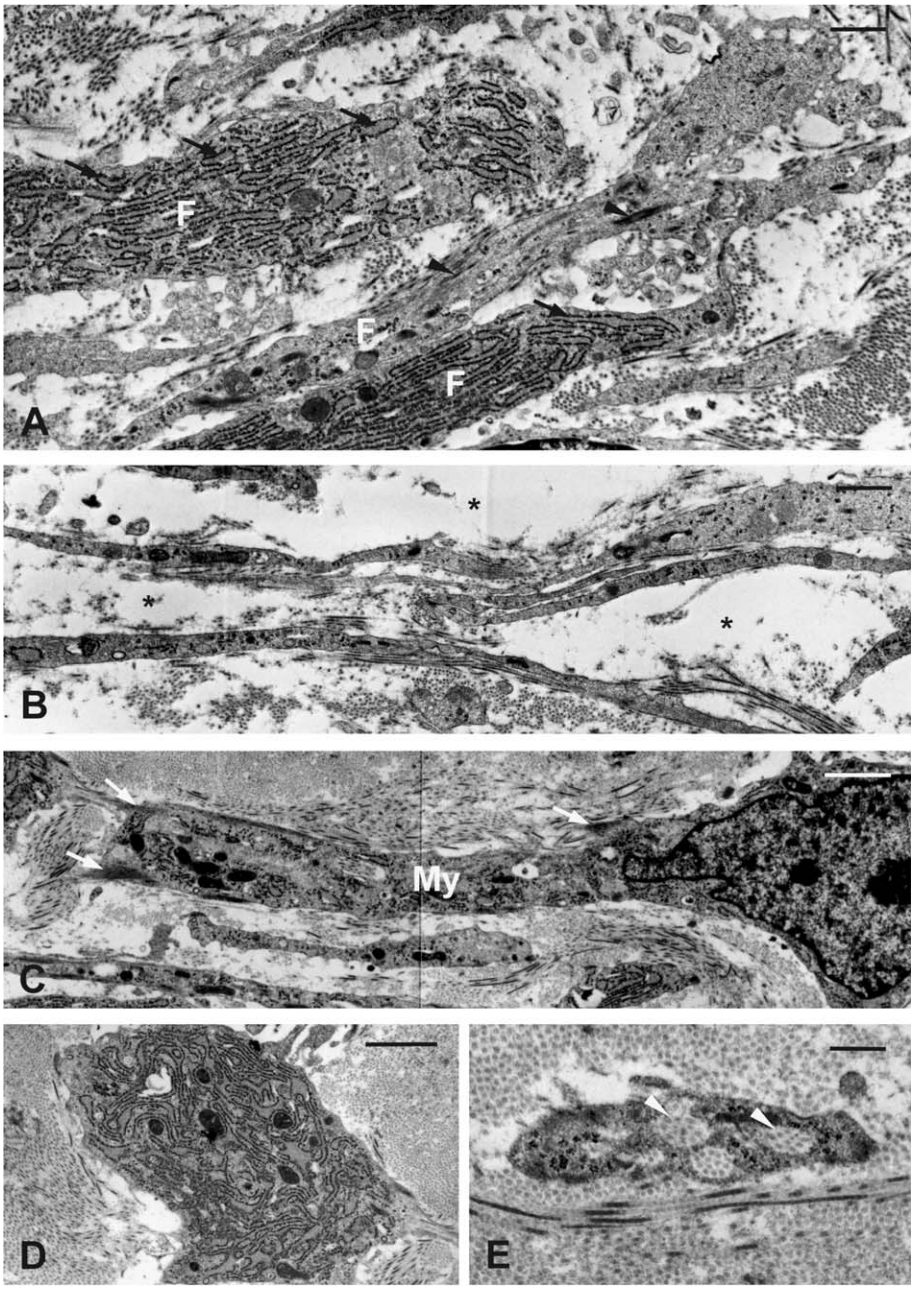

Fig. 3. (A and B) Control dermis on day 15 p.w. (A) Observe cell processes of fibroblasts (F). Some fibroblasts show abundant RER (arrow) whereas others have collagen-containing phagosomes (arrow head). In some places, short collagen fibrils form small compact bundles (compare with Fig. 2B). Bar scale: 1 μm. (B) Loose packed collagen fibrils are placed in an area occupied by an intense interstitial edema (*). Bar scale: 1 μm. (C–E) Irradiated dermis on day 15 p.w. (C) Observe a myofibroblast (My) containing abundant cytoplasmic filaments (arrows). The extracellular matrix contains unorganized collagen fibrils. Bar scale: 2 μm. (D) Fibroblast shows a well-developed RER with dilated cisternae (compare with A). Bar scale: 2 μm. (E) Fibroblasts showing many cytoplasmic recesses involving bundles of collagen fibrils (arrow head). Bar scale: 0.5 μm.

mental period. Significant differences were observed on the eighth day p.w. ($p < 0.05$). In this period, laser group showed a higher number of immunoreactive positive cells compared to control group. Despite control group had presented a higher number of positive cells than laser group on the 15th day p.w., no statistically significant differences were observed between the groups. On the 22nd day p.w., laser group showed a lower number of immunoreactive cells compared to control group ($p < 0.0001$).

3.4. Autoradiography

Quantitative evaluation of silver grains showed that in both control and irradiated-lesions the incorporation of ^{3}H-proline show a similar pattern that was lower on day 8 p.w. increased up to day 15 p.w., declining on day 22 p.w. to the same level of the eighth day p.w. (Figs. 7 and 8).

No significant difference was observed when the two groups were compared on day 8 p.w. ($p > 0.05$). However,

Please cite this article as: Carlos E.N. de Araújo et al., Ultrastructural and autoradiographical analysis show a faster ..., Journal of Photochemistry and Photobiology B: Biology (2006), doi:10.1016/j.jphotobiol.2006.08.006

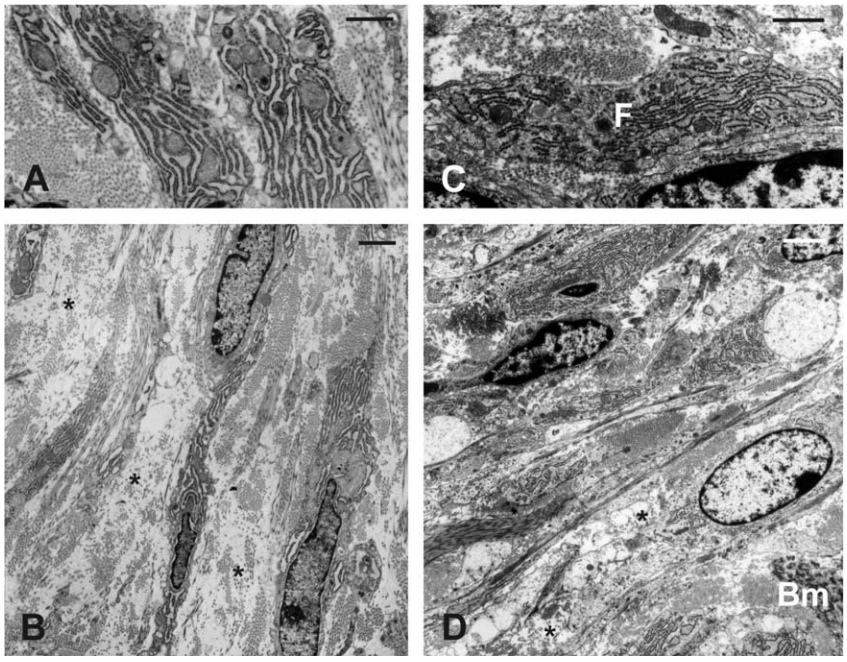

Fig. 4. (A and B) Control dermis on day 22 p.w. (A) Most fibroblasts have a well-developed RER with dilated cisternae. Bar scale: 1 μm. (B) Observe elongated fibroblasts in areas of interstitial edema (∗). Bar scale: 2 μm. (C and D) Irradiated dermis on day 22 p.w. (C) Fibroblasts (F) showing RER whose cisternae are not dilated as in control lesions (compare with Fig. 3A). Bar scale: 1 μm. (D) Note a discrete edema (∗) restrict to the subepithelial dermis (compare with Fig. 3B). Bm: basement membrane. Bar scale: 2 μm.

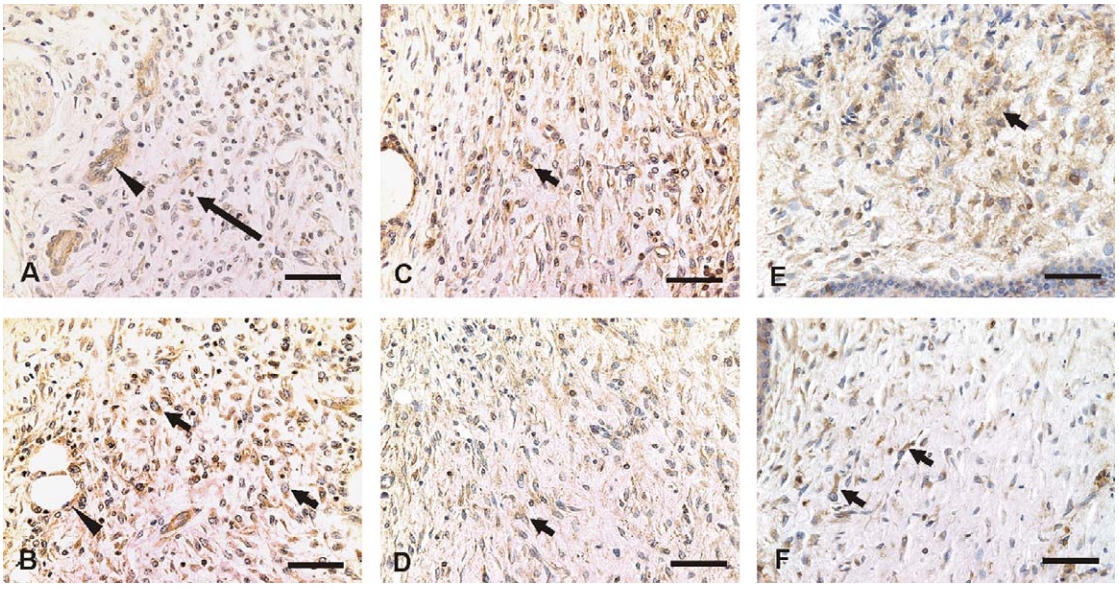

Fig. 5. (A–F) Immunohistochemistry for alpha-SMA. (A) Control dermis on day 8 p.w. Few alpha-SMA-positive cells are observed scattered between fibroblast in the dermis. Note the great number of leukocytes, particularly, neutrophils (long arrow). Muscle cells of arterioles show alpha-SMA-positive cells (long arrowhead). (B) Irradiated dermis on day 8 p.w. The number of alpha-SMA-positive cells (short arrow) is higher compared with control lesion. Note alpha-SMA-positive cells in the blood vessel wall (arrow head). (C) Control dermis on day 15 p.w. (D) Irradiated dermis on day 15 p.w. (E) Control dermis on day 22 p.w. (F) Irradiated dermis on day 22 p.w. Except for day 8 p.w., alpha-SMA-positive cells (short arrows) predominate in control samples (C and E). Bar scale: 50 μm.

although on day 15 p.w. the incorporation of ^{3}H-proline was increased in both groups, it was significantly higher in irradiated-lesions ($p < 0.05$). On the contrary, on the 22nd day p.w. although ^{3}H-proline incorporation had decreased in both groups it was significantly lower in irradiated-lesions ($p < 0.05$).

Please cite this article as: Carlos E.N. de Araújo et al., Ultrastructural and autoradiographical analysis show a faster ..., Journal of Photochemistry and Photobiology B: Biology (2006), doi:10.1016/j.jphotobiol.2006.08.006

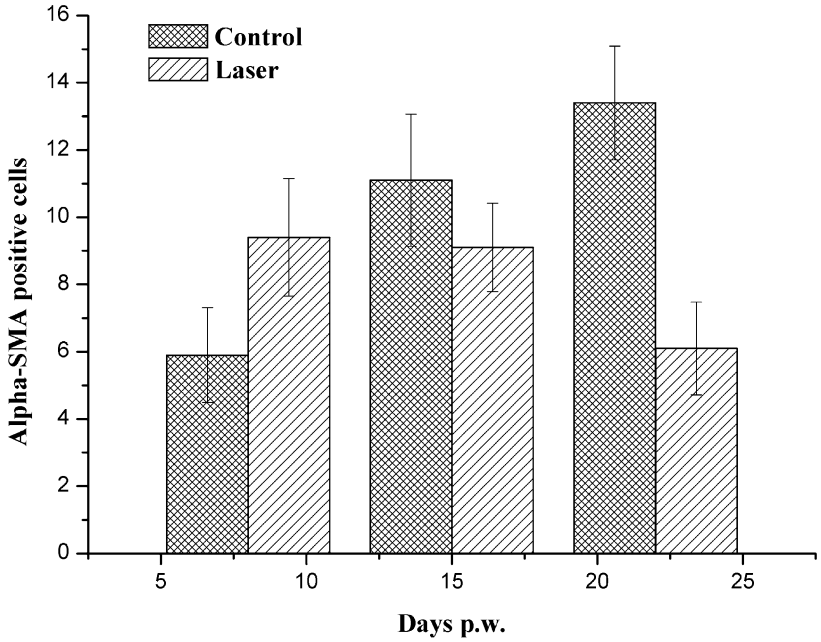

Fig. 6. Alpha-SMA-positive cells in laser and control groups. Each bar represents mean values ±SE of immunoreactive cells of 10 squares each one measuring 10,000 μm^2. Statistically significant differences were observed between laser and control group on day 8 and day 22.

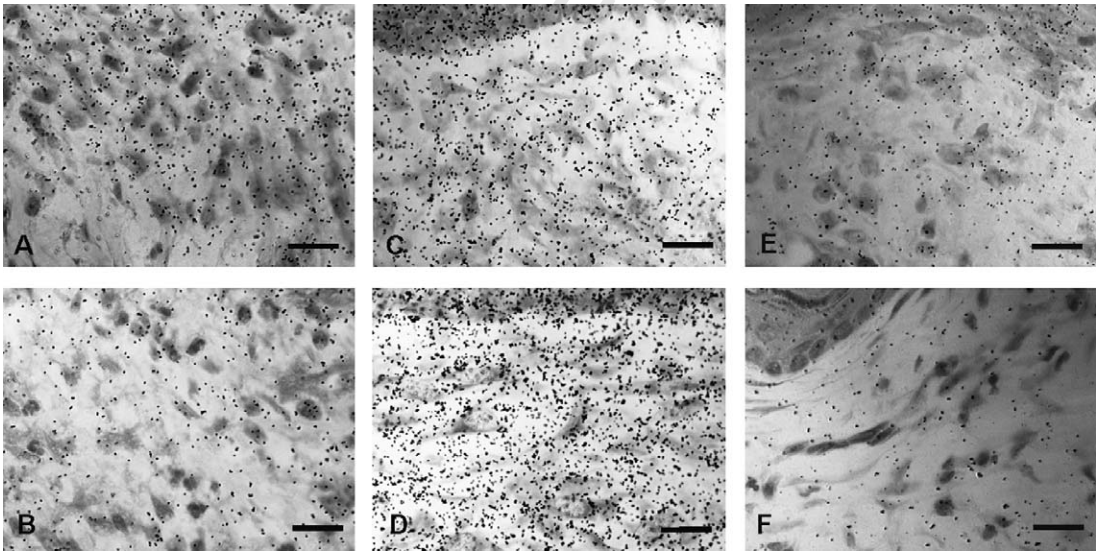

Fig. 7. Autoradiograms after ^{3}H-proline administration. (A) Control dermis on day 8 p.w. (B) Irradiated dermis on day 8 p.w. The fibroblasts are weakly labeled in both groups. (C) Control dermis on day 15 p.w. is higher labeled than day 8 p.w. (D) Irradiated dermis on day 15 p.w. show a higher ^{3}H-proline incorporation than control lesions. Compare C and D. (E) Control dermis on day 22 p.w. (F) Irradiated dermis on day 22 p.w. The incorporation of ^{3}H-proline decreases in both groups. Irradiated-lesions, however, show a lower incorporation than control lesions. Bar scale = 30 μm.

4. Discussion

We observed that the reepithelization process was faster in irradiated samples. The dermis of the irradiated wounds contained large, activated fibroblasts as well as a greater number of myofibroblasts. Moreover, fibroblasts of the irradiated-lesions showed a high number of collagen-containing phagosomes when compared with fibroblasts from the non-irradiated lesions. Apparently, the radiation inhibits the inflammatory response as observed by the precocious disappearance of neutrophils and necrosis on the first days of healing and by the lower number of macrophages and discrete interstitial edema on the later days.

A previous morphological study from our laboratory showed that the low-intensity red laser irradiation of skin burns accelerates the reepithelization leading to a faster closure of the wound [14]. Reepithelization requires a complex set of biological phenomena that include cell prolifer-

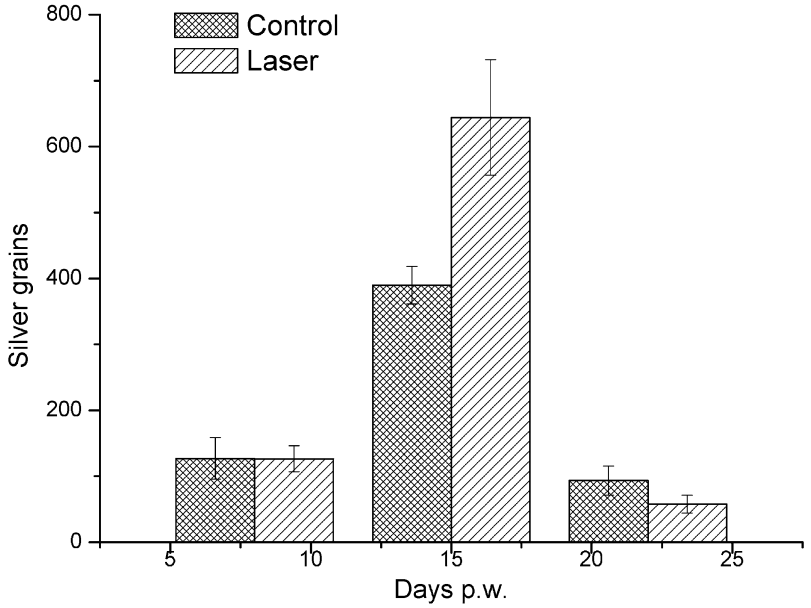

Fig. 8. ^{3}H-proline incorporation by fibroblasts of irradiated and non-irradiated skin. Each bar represents mean values ± SE of the concentration of silver grains of 20 areas counted in central repairing area. Statistically significant difference was observed between irradiated and control lesions on day 15 and day 22.

ation, cell migration and the development of new interactions with molecules of the ECM [17]. There are indications that laser radiation increases epidermal keratinocyte migration and proliferation in granulation tissues, probably by stimulating the expression of IL-1 alpha and IL-8 leading to a faster reepithelization [2].

The present study showed that He–Ne laser radiation besides stimulating reepithelization, significantly increased the number of alpha-SMA positive cells in the early stage of the healing (eighth day p.w.) compared to the control samples. However, whereas the number of myofibroblasts increased in the control dermis along the analyzed period, in the irradiated dermis the population of myofibroblasts was significantly lower than in control on day 22 p.w. Similar results were obtained in oral mucosa fibroblasts irradiated by He–Ne *in vitro* and *in vivo* [18]. During the wound healing, granulation tissue fibroblasts acquire some smooth muscle features which characterize the myofibroblasts, for review, see [19]. The role of myofibroblasts in wound contraction is well established [20,21]. Being a rich α-smooth actin filaments cell, myofibroblasts are able to contract and in this way accelerate wound closure. We may consider that the faster wound closure observed in the irradiated group in our experiment may be influenced by an increase in wound contraction promoted by myofibroblasts in the early state of the healing [22]. It is known that during the normal wound healing, myofibroblasts disappear when wound is fully reepithelized [23]. Accordingly, the number of alpha-SMA-positive cells in irradiated samples was lower than the control at 22 days post-wound.

It was notable the effect of the laser radiation on the biology of the fibroblast. Whereas fibroblasts of the irradiated samples on day 8 p.w. showed clear features of protein secretory cells, similar morphology was seen only on day 15 p.w. in the control lesion. In the irradiated skin, the majority of fibroblasts had a well-developed RER filled by electron dense material indicating a high commitment to protein synthesis and secretion. Besides synthesizing proteins, fibroblasts also possessed many collagen-containing phagosomes indicating their commitment to the degradation of damaged extracellular matrix. Phagocytosis of collagen fibrils was clearly notable in irradiated-lesions. Interestingly, in control lesions, only a few fibroblasts showed collagen-containing phagosomes and these cells did not have well-developed protein synthesis machinery suggesting a limitation of biological activity. Previous reports showed that fibroblasts work unidirectionally, that is either performing collagen synthesis or collagen degradation at any given time [24]. Our results showed that laser treated-fibroblasts are stimulated to perform both activities at the same time.

Degradation of collagen is usually done by metalloproteinase activity in the extracellular space. Phagocytosis of collagen by fibroblasts is infrequent in normal skin healing although it occurs in some tissues such as in the periodontal ligament [25] and the pregnant uterus [26], and indicates an intense remodeling of this tissue. Some reports have demonstrated that laser radiation accelerates collagen synthesis in different biological models [3,27]. The faster removal of the damaged collagen fibrils of the extracellular compartments by phagocytosis associated with less inflammatory activity and, consequently, less metalloproteinase activity may accelerate the wound healing.

The biological effect of laser radiation is not yet completely understood. According to Karu, red radiation is absorbed by chromophores of the respiratory chain, which

alter metabolism, leading to signal transduction to other parts of the cell, which finally leads to the photoresponse [28]. This effect depends on the physical characteristics of the radiation, irradiation parameters, and on the cell redox state. Recent report has showed a positive effect of He–Ne laser on healing impaired diabetic rat wounds [29]. By biomechanical and biochemical analysis the authors concluded that compared with GaAs ($\lambda = 904$ nm) laser at 1 J/cm^2, the He–Ne ($\lambda = 632.8$ nm) laser at the same dose was more efficient in promoting the wound healing in diabetic rats. Moreover, according to Pinfildi and collaborators, He–Ne laser is efficient to increase random skin flap viability in rats since laser-treated animals showed an average necrotic area lower than non-treated rats [30]. In fact, the He–Ne laser physical properties permit a high penetration in skin since its absorption by water and blood is weak. Therefore, we may consider that this wavelength is appropriated to treat open wounds [31].

Another important point is that the stimulatory effects of laser photostimulation appear to be related to specific events during the first two phases of wound healing, i.e., the inflammation phase and the proliferative phase indicating that the period of intervention may be critical [32]. For this reason, in our study, the treatment was carried out at days 1, 3, 5, 8, 12 and 15 p.w. Our experiment showed that the laser has some anti-inflammatory effect on the irradiated skin. This finding fits with Medrado and collaborators results, who reported that laser therapy reduced the inflammatory reaction in rats cutaneous wounds [33]. Quantitative autoradiography showed that ^{3}H-proline incorporation was significantly increased in the irradiated dermis on day 15 p.w. and in control dermis on the 22 day p.w. This finding strongly suggests that laser radiation influences protein synthesis by fibroblasts during the remodeling stage. Although the amino acid proline is not a specific marker for collagen, we may consider that part of this amino acid will be used for synthesizing collagen and in this way contributing to accelerate wound healing. As the animals were sacrificed one hour after the precursor injection, the autoradiographic data can be correlated with protein synthesis. In fact, our ultrastructural findings showed very developed fibroblasts in irradiated-lesions on day 15 p.w. Moreover, on day 22 p.w. the incorporation of ^{3}H-proline was diminished and correlates with a decreased of protein synthesis machinery in fibroblasts in irradiated-lesions.

On the 15th day p.w., irradiated-lesions showed compact and parallel bundles of well-organized collagen fibrils, filling the extracellular spaces. Similar organization of collagen fibrils was not observed in the control lesions at the same period. The laser radiation appears to have an influence on the fibrillogenesis of the collagen fibrils. Irradiated fibroblasts had many cytoplasmic processes, defining extracellular compartments into which groups of thin collagen fibrils were organized. Trelstad and Hayashi observed similar arrangements during fibrillogenesis in tendons of the chick embryo [34]. It is accepted that organization of collagen fibrils in bundles of parallel fibrils may increase the tensile strength of the tissue. In fact, some works showed in animal models an improved tensile strength on the irradiated skin during the repair process using a He–Ne laser [13,35]. Thus, we may consider that red laser radiation stimulates an increase in the number of cytoplasmic recesses in the fibroblasts surface and, consequently, promotes a better organization of collagen fibrils in irradiated tissues.

Considering the anti-inflammatory effect of the irradiation observed in this work, it is reasonable to hypothesize that laser radiation could influence the production of inflammatory mediators such as cytokines. The TGF-β is an important cytokine that acts during the healing process by activating cell proliferation. It is possible that the laser acts upon the macrophage respiratory chain, enhancing TGF-β production, which inhibits diapedesis of macrophages into the connective tissue. This mechanism may explain the reduced edema and number of macrophages in the irradiated dermis compared with the control dermis. The TGF-β has a high number of biological effects such as induction of differentiation of fibroblast into myofibroblasts [18,36], angiogenesis [37], stimulation of collagen synthesis [38–40] and inhibition of metalloproteinases by tissue inhibitor metalloproteinase stimulation [41]. All these biological phenomena were observed in our experiment particularly in the irradiated samples. Although this is an attractive hypothesis, there is still no evidence that laser radiation may stimulate TGF-β production *in vivo*. This hypothesis needs to be validated by further experiments.

In summary, the present study indicates that the low-intensity red laser radiation accelerates wound healing by stimulating the biological activities and differentiation of fibroblasts and by reducing the inflammatory process. Irradiation also appears to have an effect on the organization of collagen fibrils in the extracellular compartment. The beneficial effects of the laser radiation were particularly distinguishable on days 8 and 15 p.w.

Acknowledgements

We kindly thank to Dr. Alison Colquhoun for critical readings of the manuscript, Dr. Marcelo Giovannetti for the quantitative evaluation of the autoradiograms, and MSc. Renato A. Prates for the statistical analysis. The authors are grateful to Mrs. Cleusa M.R. Pellegrini for the excellent technical assistance with the preparation of the histological samples, the Immunohistochemistry as well as with the autoradiograms. This study was supported by a research grant from FAPESP (98/06784-1) and CNPq. C.E.N.A. was supported by a scholarship from FAPESP (99/00193-4).

References

[1] K.C. Smith, The photobiological basis of low level laser radiation therapy, Laser Ther. 3 (1991) 19–24.

[2] H.S. Yu, K.L. Chang, C.L. Yu, J.W. Chen, G.S. Chen, Low-energy helium–neon laser irradiation stimulates interleukin-1 alpha and interleukin-8 release from cultured human keratinocytes, J. Invest. Dermatol. 107 (1996) 593–596.
[3] G.K. Reddy, L. Stehno-Bittel, C.S. Enwemeka, Laser photostimulation accelerates wound healing in diabetic rats, Wound Rep. Regen. 9 (2001) 248–255.
[4] H. Loevschall, D. Arenholt-Bindslev, Effect of low level diode laser irradiation of human oral mucosa fibroblasts *in vitro*, Lasers Surg. Med. 14 (1994) 347–354.
[5] S.M. Ghamsari, K. Taguchi, N. Abe, J.A. Acorda, M. Sato, H. Yamada, Evaluation of low level laser therapy on primary healing of experimentally induced full thickness teat wounds in dairy cattle, Veter. Surg. 26 (1997) 114–120.
[6] I. Garavello-Freitas, V. Baranauskas, P.P. Joazeiro, C.R. Padovani, M. Pai-Silva, M.A. Cruz-Höfling, Low-power laser irradiation improves histomorphometrical parameters and bone matrix organization during tibia wound healing in rats, J. Photochem. Photobiol. B: Biol. 70 (2003) 81–89.
[7] S.M. Skinner, J.P. Gage, P.A. Wilce, R.M. Shaw, A preliminary study of the effects of laser radiation on collagen metabolism in cell culture, Aust. Dent. J. 41 (1996) 188–192.
[8] R.P. Abergel, R.F. Lyons, J.C. Castel, R.M. Dwyer, J. Uitto, Biostimulation of wound healing by lasers: experimental approaches in animal models and in fibroblast cultures, J. Dermatol. Surg. Oncol. 13 (1987) 127–133.
[9] D. Saperia, E. Gassberg, R.F. Lyons, R.P. Abergel, P. Baneux, J.C. Castel, R. Dwyer, J. Uitto, Demonstration of elevated type I and type III procollagen mRNA levels in cutaneous wounds treated with helium–neon laser, Biochem. Biophys. Res. Com. 138 (1986) 1123–1128.
[10] A. Dube, H. Bansal, P.K. Gupta, Modulation of macrophage structure and function by low level He–Ne laser irradiation, Photochem. Photobiol. Sci. 2 (2003) 851–855.
[11] H. Zheng, J.-Z. Qin, H. Xin, S.-Y. Xin, The activating action of low level helium neon laser radiation on macrophages in the mouse model, Laser Ther. 4 (1992) 55–58.
[12] G. Majno, I. Joris, Cells, Tissues and Disease. Principles of General Pathology, Blackwell Science, Cambridge, 1996.
[13] F. Lyons, R.P. Abergel, R.A. White, R.M. Dwyer, J.C. Castel, J. Uitto, Biostimulation of wound healing in vivo by a helium–neon laser, Ann. Plast. Surg. 18 (1987) 47–50.
[14] M.S. Ribeiro, D.F.T. Silva, C.E.N. Araujo, S.F. Oliveira, C.M.R. Pelegrini, T.M.T. Zorn, D.M. Zezell, Effects of low-intensity polarized visible laser radiation on skin burns: a light microscopy study, J. Clin. Laser Med. Surg. 22 (2004) 59–66.
[15] M.J. Karnovsky, A formaldehyde–glutaraldehyde fixative of high osmolarity for use in electron microscopy, J. Cell. Biol. 27 (1965) 137.
[16] S.F. Oliveira, P.A. Abrahamsohn, T. Nagata, T.M.T. Zorn, Incorporation of 3H-amino acids by endometrial stromal cells during decidualization in the mouse. An autoradiographic study, Cell. Mol. Biol. 41 (1995) 107–116.
[17] J. Gailit, R.A.F. Clark, Wound repair in the context of extracellular matrix, Curr. Opin. Cell. Biol. 6 (1994) 717–725.
[18] N. Pourreau-Schneider, A. Ahmed, M. Soudry, J. Jacquemier, F. Kopp, J.C. Franquin, P.M. Martin, Helium–neon laser treatment transforms fibroblasts into myofibroblasts, Am. J. Pathol. 137 (1990) 171–178.
[19] W. Schürch, T.A. Seemayer, G. Gabbiani, Myofibroblast, in: S.S. Sternberg (Ed.), Histology for Pathologists, Raven Press, New York, 1992, pp. 109–144.
[20] D.P. Berry, K.G. Harding, M.R. Stanton, B. Jasani, H. Ehrlich, Human wound contraction: collagen organization, fibroblasts and myofibroblasts, Plast. Reconstr. Surg. 102 (1998) 124–131.
[21] B. Hinz, G. Gabbiani, Cell-matrix and cell–cell contacts of myofibroblasts: role in connective tissue remodeling, Thromb. Haemostatis 90 (2003) 993–1002.
[22] V. Moulin, F.A. Auger, D. Garrel, L. Germain, Role of wound healing myofibroblasts on reepitheliazation of human skin, Burns 26 (2000) 3–12.
[23] A.M.A. Costa, A. Desmouliére, Mechanisms and factors involved in development of hypertrophic scars, Eur. J. Plast. Surg. 21 (1998) 19–23.
[24] T. Yajima, Localization of acid phosphatase activity in collagen-secreting and collagen-resorbing fibroblasts, Histochemistry 90 (1988) 245–253.
[25] M.T. van der Pauw, T. van den Bos, V. Everts, W.B. Beertsen, Phagocytosis of fibronectin and collagens type I, III, and V by human gingival and periodontal ligament fibroblasts in vitro, J. Periodontol. 72 (2001) 1340–1347.
[26] T.M.T. Zorn, A.T. Bijovsky, E.M. Bevilacqua, P.A. Abrahamsohn, Phagocytosis of collagen by mouse decidual cells, Anat. Rec. 225 (1989) 96–100.
[27] C.S. Enwemeka, Ultrastructural morphometry of membrane-bound intracytoplasmic collagen fibrils in tendon fibroblasts exposed to He–Ne laser beam, Tissue Cell 24 (1992) 511–523.
[28] T. Karu, Primary and secondary mechanisms of action of visible to near-IR radiation on cells, J. Photochem. Photobiol. B: Biol. 49 (1999) 1–17.
[29] G.K. Reddy, Comparison of the photostimulatory effects of visible He–Ne and infrared Ga–As lasers on healing impaired diabetic rat wounds, Lasers Surg. Med. 33 (2003) 344–351.
[30] C.E. Pinfildi, R.E. Liebano, B.S. Hochman, L.M. Ferreira, Helium-neon laser in viability of random skin flap in rats, Lasers Surg. Med. 37 (2005) 74–77.
[31] J. Tunér, L. Hode, Low Level Laser Therapy. Clinical Practice and Scientific Background, Prima Books, Grängesberg, Sweden, 1999.
[32] G.K. Reddy, Photobiological basis and clinical role of low-intensity lasers in biology and medicine, J. Clin. Laser Med. Surg. 22 (2004) 141–150.
[33] A.R.A.P. Medrado, L.S. Pugliese, S.R.A. Reis, Z.A. Andrade, Influence of low level laser therapy on wound healing and its biological action upon myofibroblasts, Lasers Surg. Med. 32 (2003) 239–244.
[34] R.L. Trelstad, K. Hayashi, Tendon collagen fibrillogenesis: intracellular subassemblies and cell surfaces changes associated with fibril growth, Dev. Biol. 71 (1979) 228–242.
[35] C.H. Halcin, J. Uitto, Biologic effects of low-energy lasers, in: K.A. Arndt, J.S. Dover, S.M. Olbricht (Eds.), Lasers in Cutaneous and Aesthetic Surgery, Lippincot-Raven, Philadelphia, 1997, pp. 303–328.
[36] A. Desmoulière, A. Geinoz, F. Gabbiani, G. Gabbiani, Transforming growth factor-β1 induces α-smooth muscle actin expression in granulation tissue myofibroblasts and in quiescent and growing cultured fibroblasts, J. Cell. Biol. 122 (1993) 103–111.
[37] P. Lievens, The influence of laser treatment on the lymphatic system and on wound healing, Med. Laser Rep. 3 (1985) 29–31.
[38] T.L. Tuan, A. Song, S. Chang, S. Younai, M.E. Nimni, In vitro fibroplasia: matrix contraction, cell growth, and collagen production of fibroblasts cultured in fibrin gels, Exp. Cell. Res. 223 (1996) 127–134.
[39] A.B. Roberts, M.B. Sporn, Peptide Growth Factors and their Receptors, Spring-Verlag, Heidelberg, 1990.
[40] S. Younai, L.S. Nichter, T. Wellisz, J. Reinisch, M.E. Nimni, T.L. Tuan, Modulation of collagen synthesis by transforming growth factor-beta in keloid and hypertrophic scar fibroblasts, Ann. Plast. Surg. 33 (1994) 148–151.
[41] J. Sodek, C.M. Overall, Matrix metalloproteinases in periodontal tissue remodeling, Matrix (Suppl. 1) (1992) 352–362.

Please cite this article as: Carlos E.N. de Araújo et al., Ultrastructural and autoradiographical analysis show a faster ..., Journal of Photochemistry and Photobiology B: Biology (2006), doi:10.1016/j.jphotobiol.2006.08.006